Design and Simulation of 77GHz Substrate Integrated Waveguide Slot Array Antenna

Bo-Yang Guo [1, 2] and Hong Jiang [1]

[1] College of Communication Engineering
Jilin University, Changchun, Jilin Province 130012, China
guoby17@mails.jlu.edu.cn, jiangh@jlu.edu.cn

[2] No. 65024 Unit, People's Liberation Army of China
Dalian, Liaoning Province 116041, China

Abstract ─ In this paper, a 77GHz slot array antenna for millimeter-wave automotive radar application is designed and simulated using HFSS, in which the substrate integrated waveguide (SIW) is adopted. First, a linear array with 16 slots is designed, and its parameters are achieved by extracting the characteristics of the radiating slot in the array environment and comparing them with the array synthesis result. Then, a tree-shaped unequal feeding network with improved vertical transition is presented to make the entire array more compact. Finally, the configuration of the designed 8 × 16 planar array antenna is given, and the fabrication error is analyzed. The simulation results of the 77GHz SIW slot array antenna show that its sidelobe levels (SLLs) are below -25dB in the E-plane and below -27dB in the H-plane, and the corresponding half-power beamwidths are 13.9° and 9.7°, respectively.

Index Terms ─ Automotive radars, feeding network, slot array antenna, substrate integrated waveguide (SIW).

I. INTRODUCTION

77GHz millimeter-wave radar enables high spatial resolution and high transmit power for a small antenna size. Also, it is robust against environmental influences such as extreme temperatures, bad light or weather conditions [1].

Recently, the 77GHz array antenna for millimeter-wave automotive radar application has drawn more and more attention. In [2] and [3], a 25×10 and a 20×16 microstrip series-fed array antennas for millimeter-wave automotive radar were deigned, respectively. However, the ideal sidelobe levels (SLLs) cannot be achieved by the radiation effect of feeding networks and their antenna sizes are large. In [4], a series-fed patch array antenna was presented, which has reduced the size and has a wide bandwidth, nevertheless, its beamwidth in elevation is large that the radar is easy to be affected by ground clutter in practical application. In general, the 3dB beamwidth in elevation is ±5 degree. In [5], a series-fed patch array antenna for 77GHz automotive radar was designed and measured, which has reduced the radiation of the feeding network, however, the effect on the radiation pattern still exists owing to the half-microstrip structure. In fact, all the above-mentioned microstrip patch antennas are not the appropriate choices as the radiation loss and dielectric loss of microstrip are relatively large in the millimeter-wave band.

Substrate integrated waveguide (SIW) is a new planar guided-wave structure fabricated in a dielectric substrate. Its guided-wave characteristic is close to that of conventional metallic waveguide [6]. It keeps both the advantages of metallic waveguide and planar microstrip structure. Waveguide slot array antennas are widely used in radar and communication systems featuring high gain, high efficiency, low cross-polarization levels and great capability of accurate control of the radiation patterns [7]. The SIW slot antenna inherits the virtues of waveguide slot antenna, and also has the advantages of low profile, compact size, low cost, and ease of being integrated with planar circuits [8]. In [9], an SIW slot array with flat-shoulder-shaped radiation pattern was designed for both medium-range radar and long-range radar applications, in which the desired radiation pattern can be obtained. However, its reliability is to be improved for simultaneous detection of two ranges in one antenna by pattern synthesis.

In this paper, we present a design of a 77GHz SIW slot array antenna for millimeter-wave automotive radar application, which is achieved via EM simulation using HFSS. It owns wide bandwidth, miniaturization, low sidelobes, narrow beams and high gain.

In the classic design of longitudinal slot array, the Elliott's iterative method is usually used, in which all the mutual coupling effects are taken into account, and the slot parameters for the desired aperture distribution and impedance matching are accurately determined with Elliott's iterative procedure [7]. However, the Elliott's

Submitted On: December 17, 2019
Accepted On: April 10, 2020

procedure is computationally complicated. With the development of the electromagnetic (EM) computation techniques, it is possible to design a slot array antenna using EM simulation software like HFSS.

Unlike the conventional Elliott's iterative method, we exploit the array synthesis result to obtain the design parameters in serial-fed array. First, we design a linear array with 16 slots and obtain its parameters by extracting the characteristics of the radiating slot in the array environment and comparing them with the array synthesis result. Then, we present a tree-shaped unequal feeding network with improved vertical transition, which can increase space utilization and reduce the entire antenna size. Finally, we design the 8 × 16 planar array antenna, and analyze the fabrication errors to test the tolerance of the antenna.

II. DESIGN OF LINEAR ARRAY

The design parameters need to meet the requirements of certain amplitude distribution and impedance matching when we design an SIW linear array with slots. Its design procedure is as follows: The first step is to extract the radiating characteristics of the radiation element, which is the relationship of the slot normalized resonant conductance against resonant slot length and slot offset. The next step is to obtain the excitation amplitude distribution from the array synthesis result, and according to the distribution, the normalized conductance of each slot is determined. The final step is to obtain the design parameters of each slot by comparing it with the characteristic curve of slot.

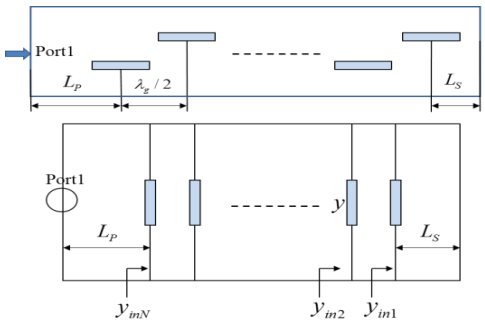

Fig. 1. Slotted waveguide and its equivalent circuit.

According to the principle of the slot characteristics extraction [10], a waveguide with N slots and its equivalent circuit can be shown in Fig. 1. The distance from the first slot to the short-circuit matching stub and the distance from the last slot to the input port are L_s and L_p, respectively.

According to the transmission line theory, for a transmission line of length L_s with an arbitrary load, its normalized input admittance is:

$$y_{in}(L_s)=\frac{y_l+j\tan(\beta L_s)}{1+jy_l\tan(\beta L_s)}, \tag{1}$$

where y_l denotes the normalized admittance of load. When the transmission line has a short-circuit load as in Fig. 1, (1) can be rewritten as:

$$y_{in}(L_s)=\frac{1}{j\tan(\beta L_s)}. \tag{2}$$

The lengths and offsets of all slots are set to be the same, consequently, the admittance of every slot can be assumed with an identical value y. Thus, for the 1st slot, the normalized input admittance y_{in1} can be expressed as:

$$y_{in1}=\frac{1}{j\tan(\beta L_s)}+y. \tag{3}$$

Similarly, y_{in2} and y_{inN} can be derived as:

$$y_{in2}=\frac{y_{in1}+j\tan(\beta\frac{\lambda_g}{2})}{1+jy_{in1}\tan(\beta\frac{\lambda_g}{2})}+y, \tag{4}$$

$$y_{inN}=\frac{y_{inN-1}+j\tan(\beta\frac{\lambda_g}{2})}{1+jy_{inN-1}\tan(\beta\frac{\lambda_g}{2})}+y. \tag{5}$$

As the distance from the Nth slot to the input port is L_p, the input admittance at the input port of waveguide can be expressed as:

$$y_{in}=\frac{y_{inN}+j\tan(\beta L_p)}{1+jy_{inN}\tan(\beta L_p)}. \tag{6}$$

In addition, the normalized input admittance can be also computed from the reflection coefficient [10], i.e.,

$$y_{in}=\frac{1-\Gamma_{11}e^{j2\beta L_p}}{1+\Gamma_{11}e^{j2\beta L_p}}+j\cot(\beta L_s), \tag{7}$$

where Γ_{11} equals to S_{11}, and $\beta=2\pi/\lambda_g$, λ_g is the guided wavelength in equivalent waveguide. Here, when $L_p=2\lambda_g, L_s=\lambda_g/4$, we can have:

$$y_{inN}=y_{in}=\frac{1-S_{11}}{1+S_{11}}. \tag{8}$$

Therefore, the relationship can be established between S_{11} of the input port and total normalized admittance of all slots. The only unknown parameter in (8) is S_{11} of the slotted waveguide, which can be obtained by simulation via HFSS. Then the normalized admittance of every single slot can be calculated by:

$$y=\frac{1-S_{11}}{N(1+S_{11})}, \tag{9}$$

where N is the number of slots in array.

In our design, the slot characteristics extraction procedure is carried out in a 5×16 array model as shown in Fig. 2, in which all the mutual coupling effects in the array environment are taken into account as much as possible.

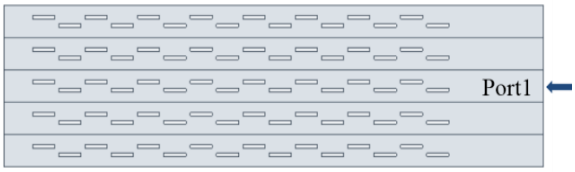

Fig. 2. Equivalent slotted array model for slot characteristics extraction via HFSS.

For parameter extraction, an equivalent dielectric-filled rectangular waveguide model is used according to the SIW equivalent theory to reduce the HFSS meshing and simulation time [11]. The equation of the equivalent width can be expressed as:

$$a_{RWG} = a - 1.08\times\frac{d^2}{p} + 0.1\times\frac{d^2}{a}, \tag{10}$$

where a_{RWG} denotes the width of equivalent rectangular waveguide, and a, d, p denotes the width of the SIW, the period and diameter of the via, respectively.

In the extracting procedure, the slot length is optimized at various offsets. All slots can be considered as in resonance state when the objective function $\mathrm{Im}(S_{11})=0$. By recording the slot length and S_{11} at this point, the resonant lengths and normalized conductance versus various slot offset can be obtained. We can use MATLAB to fit the relationship curve of them. The fitting curves are shown in Fig. 3.

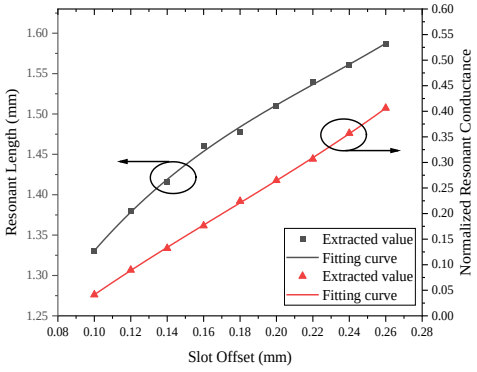

Fig. 3. Characteristic curve of radiating slot.

A certain design margin should be provided for processing in our design and simulation, in order to accommodate unexpected dimension variations in fabrication procedure. A relative strict SLLs standard of -30dB Taylor distribution is adopted for the synthesis in H-plane pattern. The normalized conductance of *n*th slot can be calculated by:

$$g_n = \frac{U_n^2}{\sum_{n=1}^{N} U_n^2}, \tag{11}$$

where U_n is the *n*th element's excitation amplitude from the synthesis. When the normalized conductance of each slot is obtained, the design parameter (length and offset) of each slot can be obtained by comparing it with the slot characteristic curve. The configuration of the SIW slot linear array is shown in Fig. 4.

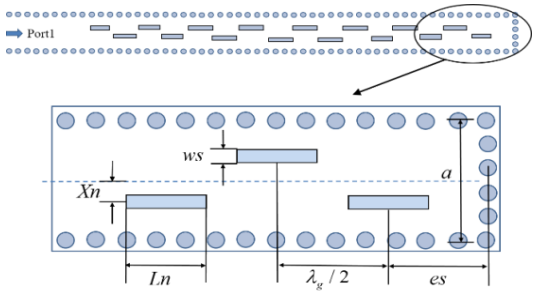

Fig. 4. Configuration of the SIW slot linear array.

In Fig. 4, the width of SIW is 2.3mm, the diameter of the metallized via is 0.4mm, and the distance between two adjacent vias is 0.6mm. The distance between adjacent longitudinal slots is one-half guide wavelength, and the short-circuit matching stub distance is a three-quarter guided wavelength. The liner array is designed on Rogers 5880 dielectric substrate with relative dielectric constant $\varepsilon_r = 2.2$ and thickness 0.508mm. Further optimization is usually required since the simulation results by the initial design parameters are often not perfect. The final optimized design parameters are listed in Table 1.

Table 1: Design parameters of the linear array

Parameter	Value (mm)	Parameter	Value (mm)
L_1	1.3	X_1	0.09
L_2	1.3	X_2	-0.09
L_3	1.31	X_3	0.1
L_4	1.33	X_4	-0.1
L_5	1.36	X_5	0.1
L_6	1.38	X_6	-0.12
L_7	1.4	X_7	0.14
L_8	1.41	X_8	-0.14
es	2.95	*ws*	0.2

The simulation results of S_{11} and radiation patterns of the linear array are shown in Fig. 5 and Fig. 6. The optimized results show that S_{11} is below -10 dB from

76GHz to 78.3GHz, and a relative bandwidth of 2.99% is achieved, with the gain of 15.3 dBi at 77GHz. The half-power beamwidth (HPBW) of the H-plane pattern is 8.9°, and the SLLs are lower than -26 dB. Therefore, the design of SIW serial-fed slot linear array has achieved good performance and will be used as the sub-array of planar array in the next step.

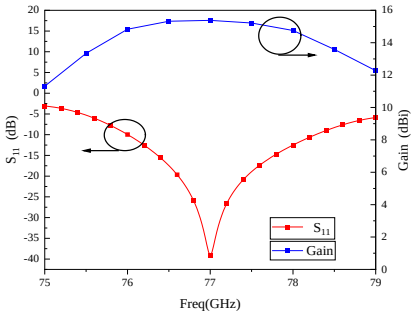

Fig. 5. Simulated S_{11} of the linear array.

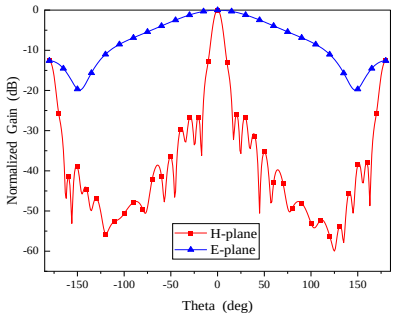

Fig. 6. Simulated radiation patterns of the linear array.

III. DESIGN OF FEEDING NETWORK

Based on the previous design of the linear array, an 8×16 planar array antenna can be designed, in which an eight-way tree-shaped unequal feeding network with transition is required to excite the eight sub-arrays with tapered amplitude and in-phase output.

A. Transition between RWG and SIW

As the transmission loss of coaxial line in millimeter-wave band is relatively large, a transition from rectangular waveguide (RWG) to SIW is generally used as the feed. The commonly-used waveguide-SIW transition is a vertical transition one [12]. A coupling aperture with the size smaller than the waveguide inner wall is etched on the broadside of a slightly wider SIW, which is called the step-SIW, and the standard waveguide is vertically fixed to the coupling aperture. Impedance matching is achieved by adjusting the size of the step-SIW and coupling aperture.

In this section, we first simulate a conventional RWG-SIW transition according to [12], whose configuration and simulated S-parameters results are shown in Fig. 7 and Fig. 8, respectively. The feeding waveguide employed here is a WR-10 waveguide with inner wall sizes 2.54mm and 1.27mm, respectively. The simulation results show that a 12% bandwidth (69.4GHz-78.5GHz) is achieved with $S_{11} < -15dB$ and insert loss lower than 0.3 dB, which can provide smooth transition from RWG to SIW.

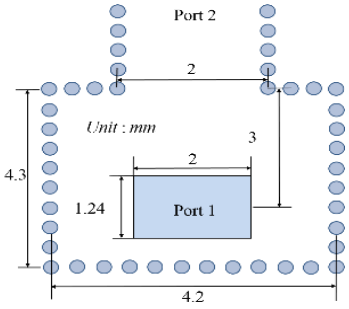

Fig. 7. Configuration of the conventional RWG-SIW transition.

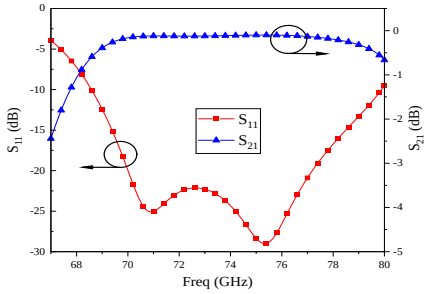

Fig. 8. Simulated S-parameters of the conventional transition.

B. Design of eight-way feeding network with improved vertical transition

The feeding network usually consists of a tree-shaped power divider and a vertical transition. The conventional and proposed feeding networks are shown in the left and right sides of Fig. 9, respectively.

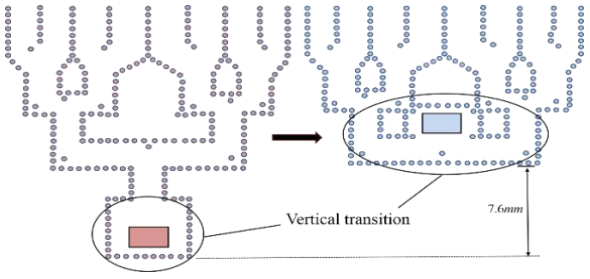

Fig. 9. Configuration of conventional and proposed feeding network.

As shown in Fig. 9, the vertical transition of the conventional feeding network is separately placed below the power divider, and it requires to pass through a certain length's SIW transmission line to achieve stable transmission before connecting to the power divider. Clearly, it makes the feeding network not compact enough. Besides, there is an idle area above the first T-junction, and the space utilization is too low.

We propose a feeding network with improved vertical transition. The configuration of the novel feeding structure is shown in Fig. 10, in which the vertical transition is integrated in the idle area of power divider. The size of the coupling aperture and the width of the step-SIW can refer to the design results of the transition in Section III-A. The upper-wall's distance can be obtained through simple optimization.

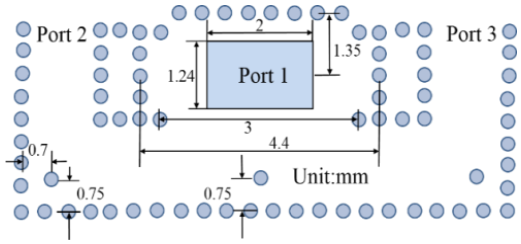

Fig. 10. Configuration of the improved transition.

The HFSS model measurement shows that by this change, the geometry of power divider has reduced from 18.5mm×18.4mm to 10.9mm×18.4mm, which has a 40% reduction. Furthermore, the original idle area is reutilized, thus the space utilization has increased.

The improved transition is next to a T-junction which has an equal power dividing ratio to the port 2 and port 3. The simulation result of S-parameters with this structure is shown in Fig. 11, it can be seen that a 16% bandwidth (70.6GHz-82.6GHz) is achieved with $S_{11} < -15dB$ and insert loss lower than 0.4 dB, which validates that the proposed transition can provide smooth transition to the SIW feeding network.

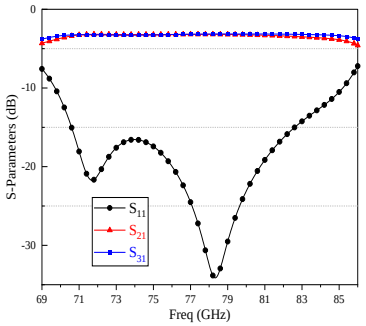

Fig. 11. Simulated S-parameters of the improved transition.

To achieve the low SLLs in the E-plane, eight ways in-phase and tapered amplitude output are required. As with the linear array, a design margin is provided for processing, and -30 dB Taylor distribution is adopted for the synthesis in E-plane pattern. The power divider is needed to divide into three stages, consisting of three T-junctions, four Y-junctions with different power dividing ratios and in-phase output, and six L-junctions at each corner to suppress reflection. These structures need to be designed separately.

The configurations of Y-junction and T-junction with uneven power dividing ratio are shown in Fig. 12. By adjusting the position of the matching via, we can improve the power reflection [13] and control the power dividing ratio, while the phase shift can be slightly tuned by adjusting the width of SIW branch [14], as different widths of SIW have different phase constants [15].

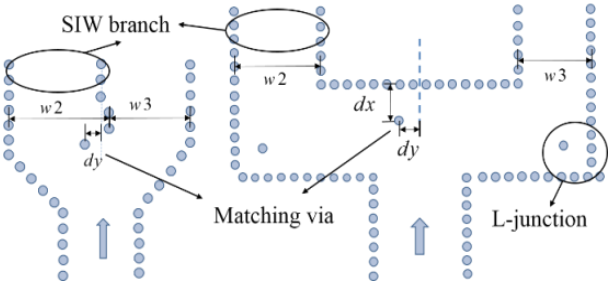

Fig. 12. Configurations of Y-junction and T-junction with a certain dividing power ratio.

We combine the optimized Y-junctions and T-junctions of each stage together to form the power divider and simulate in HFSS. Simulation results of the amplitude and phase characteristics of the complete eight-way feeding network are shown in Fig. 13 and Fig. 14. The results show that the output power dividing ratio of eight ports at 77GHz basically meets the desired goal, and the output phase error is ± 3.5 degree, which can be regarded as in-phase output.

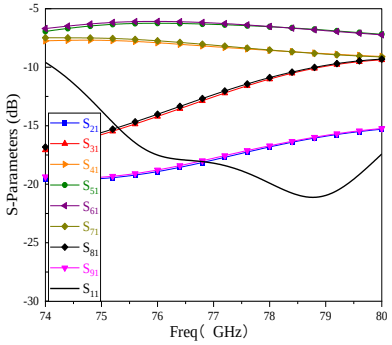

Fig. 13. Simulated amplitude characteristics of the eight-way feeding network.

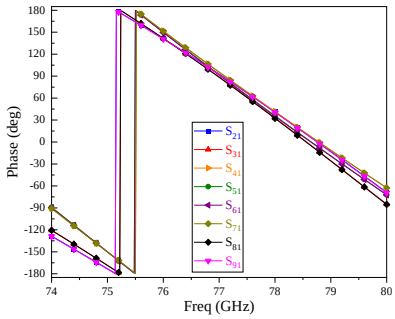

Fig. 14. Simulated phase characteristics of the eight-way feeding network.

IV. DESIGN OF 8×16 PLANAR ARRAY

The configuration of the designed 8×16 SIW slot planar array is shown in Fig. 15. The waveguide feeding port is located on the back of the antenna. The performance simulation results of the antenna are shown in Fig. 16-Fig. 19.

It can be seen from simulation results that S_{11} is below -10 dB from 76.4GHz to 78.2GHz, a relative bandwidth of 2.34% is achieved, with the gain of 23.6 dBi at 77GHz. The E-plane pattern has a half-power beamwidth of 13.9° at 77GHz, the SLLs are lower than -25 dB, and the H-plane's beamwidth is 9.7°, the SLLs are lower than -27 dB. Good performance has been achieved such as low SLLs, narrow beams and high gain.

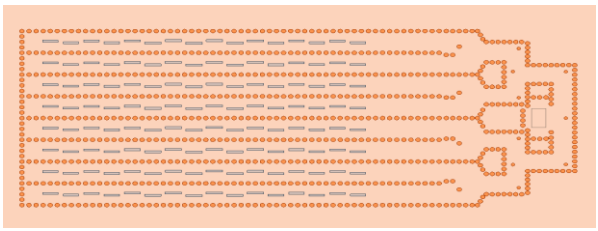

Fig. 15. Configuration of the 8×16 SIW slot array antenna.

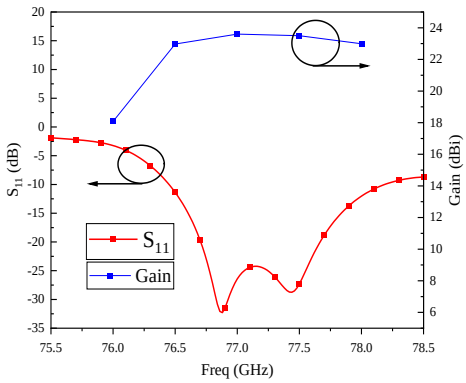

Fig. 16. Simulated S_{11} and gain of the designed antenna.

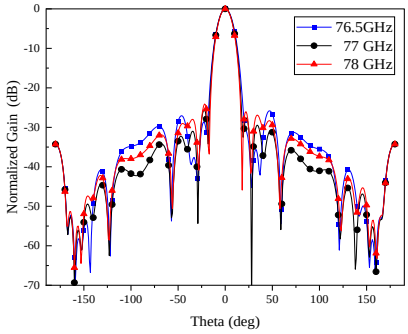

Fig. 17. Simulated E-plane patterns of the designed antenna.

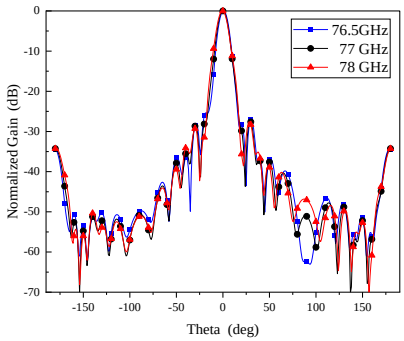

Fig. 18. Simulated H-plane patterns of the designed antenna.

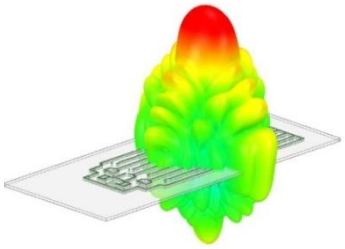

Fig. 19. 3D beam pattern of the designed antenna.

V. ERROR ANALYSIS

In the millimeter-wave band, the performance of device is very sensitive to its dimension. When the antenna is fabricated, a tiny change of design dimension may greatly affect the antenna performance. It is necessary to perform an error analysis to test the tolerance of the antenna.

Considering that the error analysis of the entire antenna will significantly increase the complexity and time consumption, the analysis is carried out in SIW linear array, in which the length error and offset error of radiation slots are taken into account and their impact on performance is analyzed and discussed, respectively.

Generally, the machining error is controlled within ±0.02mm. Therefore, the error analysis of 16 slots in

linear array can be divided into the following four cases [16]: all slots in positive tolerance, i.e., +0.02mm, all slots in negative tolerance, i.e., -0.02mm, half of them in positive tolerance with half in negative tolerance and all in random tolerance.

The impact of length error and offset error on H-plane pattern are shown in Fig. 20 and Fig. 21. We can see that the length or offset error will worsen the pattern slightly, mainly reflected in the elevation of sidelobes of 1-2 dB and the broadening of the beamwidth within 1 degree. In general, the H-plane pattern is still in good performance. The length or offset error will cause the shift of resonance point, as shown in Fig. 22 and Fig. 23. This is because that the lengths and offsets in the design are obtained from the slot characteristic curves extracted in the resonance state, and the change of length or offset will inevitably lead to the change of resonance state.

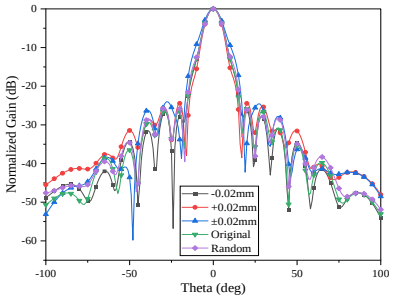

Fig. 20. Impact of length error on H-plane pattern.

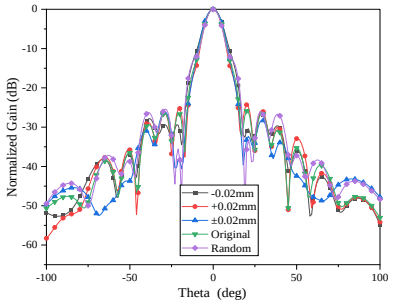

Fig. 21. Impact of offset error on H-plane pattern.

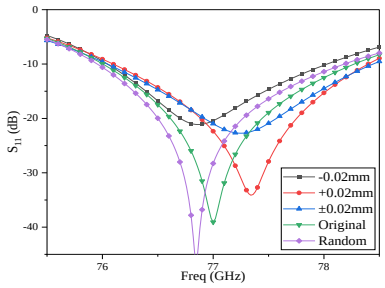

Fig. 22. Impact of length error on S_{11}.

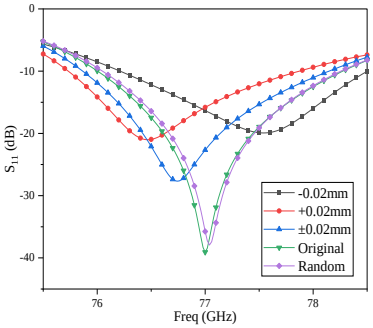

Fig. 23. Impact of offset error on S_{11}.

It can be seen from Fig. 20 to Fig. 23 that the linear array basically keeps good performance in a certain range of errors, so we can infer that the complete antenna should also have a certain tolerance. In addition, it shows that in order to achieve good performance, it is necessary to provide a certain design margin in the design process, and it's better to choose the manufacturing technology with high precision in the future.

VI. CONCLUSION

A 77GHz SIW slot array antenna is designed and simulated using the high-frequency simulation software HFSS in this paper. First, the radiating characteristic parameters of the slot are extracted using an equivalent array model, and a linear slot array with low SLLs in H-plane is designed, then an 8 × 16 planar array fed by a novel tree-shaped feeding network is designed with an improved vertical transition, which can increase the space utilization and reduce the antenna size. The fabrication errors are also analyzed to test the tolerance of the antenna. Simulation results show that the designed antenna array has the characteristics of wide bandwidth, miniaturization, low sidelobes, narrow beams and high gain. It can be served as the transmitting antenna for automotive radar applications.

REFERENCES

[1] J. Hasch, E. Topak, R. Schnabel, et al., "Millimeter-wave technology for automotive radar sensors in the 77GHz frequency band," *IEEE Transactions on Microwave Theory and Techniques*, vol. 60, no. 3, pp. 845-860, Mar. 2012.

[2] Q. Zhang, L. Wang, and X. Zhang, "Millimeter-wave microstrip comb-Line antenna array for automotive radar," *2018 12th International Symposium on Antennas, Propagation and EM Theory (ISAPE)*, pp. 1-3, Hangzhou, China, 2018.

[3] C. Yi and W. B. Dou, "Microstrip series fed antenna array for millimeter wave automotive radar applications," *2012 IEEE MTT-S International Microwave Workshop Series on Millimeter Wave*

Wireless Technology and Applications, pp. 1-3, Nanjing, 2012.

[4] X. Shang, F. Zhang, R. He, and H. Zhang, "A 77GHz miniaturized microstrip antenna array for automotive radar," *2019 International Conference on Microwave and Millimeter Wave Technology (ICMMT)*, pp. 1-3, Guangzhou, China, 2019.

[5] J. Xu, W. Hong, H. Zhang, et al., "Design and measurement of array antennas for 77GHz automotive radar application," *2017 10th UK-Europe-China Workshop on Millimetre Waves and Terahertz Technologies (UCMMT)*, Liverpool, UK, Sept. 11-13, 2017.

[6] M. Bozzi, A. Georgiadis, and K. Wu, "Review of substrate-integrated waveguide circuits and antennas," *IET Microwaves, Antennas & Propagation*, vol. 5 , no. 8 , pp. 909-920, June 2011.

[7] J. F. Xu, W. Hong, P. Chen, et al., "Design and implementation of low sidelobe substrate integrated waveguide longitudinal slot array antennas," *IET Microwaves, Antennas & Propagation*, vol. 3 , no. 5, pp. 790-797, Aug. 2009.

[8] S. Moitraa and P. S. Bhowmik, "Effect of various slot parameters in single layer substrate integrated waveguide (SIW) slot array antenna for Ku-Band applications," *The Applied Computational Electromagnetics Society (ACES) Journal*, vol. 30, no.8, pp. 934-939, Aug. 2015.

[9] Y. Yu, W. Hong, H. Zhang, et al., "Optimization and implementation of SIW slot array for both medium- and long-range 77 GHz automotive radar application," *IEEE Transactions on Antennas & Propagation*, vol. 66, no. 7, pp. 3769-3774, July 2018.

[10] M. Q. Qi, W. Wang, M. P. Jin, "A method of calculating admittance of waveguide slot," *2005 Asia-Pacific Microwave Conference Proceedings*, Suzhou, China, Dec. 4-7, 2005.

[11] F. Xu and K. Wu, "Guided-wave and leakage characteristics of substrate integrated waveguide," *IEEE Transactions on Microwave Theory & Techniques*, vol. 53, no.1, pp. 66-73, 2005.

[12] K. D. Wang, W. Hong, and K. Wu, "Broadband transition between substrate integrated waveguide (SIW) and rectangular waveguide for millimeter-wave applications," *Applied Mechanics & Materials*, vol. 130-134, pp. 1990-1993, 2012.

[13] A. Piroutiniya and P Mohammadi, "The substrate integrated waveguide T-junction power divider with arbitrary power dividing ratio," *The Applied Computational Electromagnetics Society (ACES) Journal*, vol. 31, no.4, pp. 428-433, Apr. 2016.

[14] J. Wang and Y. J. Cheng, "W-band hybrid unequal feeding network of waveguide and substrate integrated waveguide for high efficiency and low sidelobe level slot array antenna application," *International Journal of Antennas and Propagation*, vol. 2017, Article ID 7183434, 8 pages, 2017.

[15] Y. J. Cheng, W. Hong, and K. Wu, "Broadband self-compensating phase shifter combining delay line and equal-length unequal-width phaser," *IEEE Transactions on Microwave Theory & Techniques*, vol. 58, no. 1, pp. 203-210, 2010.

[16] R. Liu, "W-band waveguide slot array antenna design," *A Master Thesis from University of Electronic Science and Technology of China*, 2015.

Bo-Yang Guo received the B.S. degree in Communication Engineering from Information Engineering University, China, in 2012. He is currently a graduate student at College of Communication Engineering, Jilin University, China. His current research interest is antenna design and EM simulation.

Hong Jiang received the Ph.D. degree in Communication and Information System from Jilin University, China, in 2005. From 2010 to 2011, she was a Visiting Scholar with the Department of Electrical and Computer Engineering, McMaster University, Hamilton, ON, Canada. She is currently a Professor at the College of Communication Engineering, Jilin University, China. She is a member of Institute of Electrical and Electronics Engineers (IEEE) and senior member of the Chinese Institute of Electronics (CIE). Her research fields focus on array signal processing, radar signal processing and antenna design.